



Cloud condensation nuclei (CCN) activity of aliphatic amine secondary aerosol

X. Tang^{1,2,*}, D. Price^{1,2}, E. Praske^{3,**}, D. N. Vu^{1,2}, K. Purvis-Roberts³, P. J. Silva^{4,5}, D. R. Cocker III^{1,2}, and A. Asa-Awuku^{1,2}

¹Department of Chemical and Environmental Engineering, Bourns College of Engineering, University of California, Riverside, CA 92521, USA

²Bourns College of Engineering, Center for Environmental Research and Technology (CE-CERT), Riverside, CA 92507, USA

³W.M. Keck Science Department of Claremont McKenna, Pitzer, and Scripps Colleges, 925 N. Mills Ave., Claremont, CA 91711, USA

⁴USDA-ARS, 230 Bennett Lane, Bowling Green, KY 42104, USA

⁵Department of Chemistry and Biochemistry, 0300 Old Main Hill, Utah State University, Logan, UT 84322-0300, USA

* now at: Department of Civil and Environmental Engineering, University of California, Berkeley, USA

** now at: Division of Chemistry and Chemical Engineering, California Institute of Technology, Pasadena, CA 91125, USA

Correspondence to: A. Asa-Awuku (akua@enr.ucr.edu)

Received: 26 September 2013 – Published in Atmos. Chem. Phys. Discuss.: 2 January 2014

Revised: 7 April 2014 – Accepted: 10 April 2014 – Published: 17 June 2014

Abstract. Aliphatic amines can form secondary aerosol via oxidation with atmospheric radicals (e.g., hydroxyl radical and nitrate radical). The particle can contain both secondary organic aerosol (SOA) and inorganic salts. The ratio of organic to inorganic materials in the particulate phase influences aerosol hygroscopicity and cloud condensation nuclei (CCN) activity. SOA formed from trimethylamine (TMA) and butylamine (BA) reactions with hydroxyl radical (OH) is composed of organic material of low hygroscopicity (single hygroscopicity parameter, κ , ≤ 0.25). Secondary aerosol formed from the tertiary aliphatic amine (TMA) with N_2O_5 (source of nitrate radical, NO_3) contains less volatile compounds than the primary aliphatic amine (BA) aerosol. As relative humidity (RH) increases, inorganic amine salts are formed as a result of acid–base reactions. The CCN activity of the humid TMA– N_2O_5 aerosol obeys Zdanovskii, Stokes, and Robinson (ZSR) ideal mixing rules. The humid BA + N_2O_5 aerosol products were found to be very sensitive to the temperature at which the measurements were made within the streamwise continuous-flow thermal gradient CCN counter; κ ranges from 0.4 to 0.7 dependent on the instrument supersaturation (ss) settings. The variance of the measured aerosol κ values indicates that simple ZSR rules cannot be applied to the CCN results from the primary

aliphatic amine system. Overall, aliphatic amine aerosol systems' κ ranges within $0.2 < \kappa < 0.7$. This work indicates that aerosols formed via nighttime reactions with amines are likely to produce hygroscopic and volatile aerosol, whereas photochemical reactions with OH produce secondary organic aerosol of lower CCN activity. The contributions of semivolatile secondary organic and inorganic material from aliphatic amines must be considered for accurate hygroscopicity and CCN predictions from aliphatic amine systems.

1 Introduction

Atmospheric aerosol can influence climate directly by absorbing and scattering light and indirectly via their ability to act as cloud condensation nuclei (CCN) and influence cloud formation. Secondary aerosol, formed from oxidation reactions with gaseous precursors, is an important contributor to aerosol mass and CCN number. The relative contribution of inorganic/organic components plays a vital role in the determination of bulk CCN activity of ambient aerosol.

The ambient aerosol composition is complex. Approximately 25–50% of fine particle mass is comprised of inorganic compounds (Gray et al., 1986), such as ammonium

sulfate, nitrate, sea salt, and wind-blown dust. Organics make up ~20–90% of the global aerosol composition in the troposphere (Kanakidou et al., 2005). Only a small fraction of the organic composition has been speciated and quantified using gas chromatography with mass spectrometry (Finlayson-Pitts and Pitts, 1986; Rogge et al., 1993; Saxena and Hildemann, 1996). Thus aerosol physical and thermodynamic properties are difficult to predict with little to no information about particle chemical speciation. Therefore, parameterizations are used to effectively represent the water uptake potential of atmospheric aerosols.

The hygroscopicity parameter (Petters and Kreidenweis, 2007), κ , has been frequently used in recent studies to describe the nature of complex aerosol (e.g., Moore et al., 2012; Mikhailov et al., 2013; Tang et al., 2012; Asa-Awuku et al., 2011; Jimenez et al., 2009). Application of κ allows direct evaluation of aerosol CCN activity by combining aerosol properties, such as density, molecular weight and surface tension. Hygroscopicity values representative of atmospheric particulate matter range within $0.1 < \kappa < 0.9$ (Petters and Kreidenweis, 2007) using previous ambient studies (Fitzgerald et al., 1982; Hudson and Da, 1996; Dusek et al., 2006). Ammonium sulfate and nitrate are abundant highly soluble and hygroscopic inorganic aerosol with κ equal to 0.6 and 0.67, respectively, whereas moderately hygroscopic organic species have CCN activities corresponding to $0.01 < \kappa < 0.5$ (Petters and Kreidenweis, 2007). This wide range indicates that there is large variability in ambient aerosol composition as well as in the relative contribution of soluble and insoluble components.

Due to the common impression of most low-molecular-weight amines being highly volatile, little attention has been devoted to the gas–particle-phase partitioning of amine-containing aerosol. Sources of aliphatic amines include combustion, biomass burning, agricultural practices (e.g., vegetation, animal husbandry), and the ocean (reviewed in Ge et al., 2011a). The ambient concentration of amine can be as much as 14–23% of that of ammonia even in the presence of ammonia (Sorooshian et al., 2008). To date few studies have examined the CCN activity of amine aerosol formed from reactions with atmospheric oxidants or nitric acid. Particle phase amines have been repeatedly detected in field campaigns at different locations (summarized by Ge et al., 2011a). Recent chamber studies have confirmed both acid–base reactions and oxidation processes can lead to the formation of amine secondary aerosol (Silva et al., 2008; Murphy et al., 2007; Malloy et al., 2009b). Amines may also enhance or affect particle nucleation and the growth of nucleated particle to CCN-relevant sizes (Loukonen et al., 2010; Berndt et al., 2010; Wang et al., 2010a, b). The solubility of multiple aliphatic aminium nitrates has been summarized in Table 5 in Ge et al. (2011b), which is comparable with or higher than that of ammonium nitrate. The presence of particulate amines has been reported to be coincident with enhanced water uptake of aerosol from a bovine source (Sorooshian

et al., 2008); it can be hypothesized that aminium nitrates are highly hygroscopic, similar to ammonium nitrate. Thus, the presence of aminium nitrate salts in the ambient aerosol has the potential to impact regional air quality and CCN number concentrations.

This work focuses on the CCN behavior of trimethylamine (TMA, C_3H_9N) and butylamine (BA, $C_4H_{11}N$) secondary aerosols formed during daytime and nighttime atmospheric reactions. TMA is a tertiary amine precursor known to form secondary organic aerosol (SOA) with hydroxyl radical (OH), ozone (O_3) (Murphy et al., 2007) and nitrate radical (NO_3) (Silva et al., 2008). Ambient studies show that mass of TMA particle phase amines is dependent on relative humidity (RH; Glagolenko and Phares, 2004; Zhang et al., 2012; Rehbein et al., 2011; Tang et al., 2013). BA is a primary aliphatic amine that is less atmospherically abundant than TMA, but it has been detected at high concentrations near dairies, with concentration up to 187 ppb (Rabaud et al., 2003). Tang et al. (2013) reported the aerosol formation potential and the chemical nature (inorganic/organic) of the two aliphatic amines (TMA and BA). Tang et al. (2013) also discussed the effect of environmentally relative humidity on the reaction pathway and aerosol composition. Here we investigate the CCN activity of aerosol formed from dry and humid reactions with NO_3 and OH.

2 Experimental setup and instrumentation

Three series of experiments were conducted for both TMA and BA: OH photooxidation, NO_3 -initiated, and acid–base reactions. The initial concentration of each reactant in the experiment was as follows: precursor amine (TMA or BA) 100 ppb, HNO_3 ~ 300 ppb, N_2O_5 (nitrate radical precursor) 300 ppb, or H_2O_2 (OH precursor) 1 ppm. Both dry and humid (relative humidity < 40%) experiments were conducted for reactions between amine and OH/ NO_3 . All experiments were conducted in the 12 m³ environmental reactor chamber at the Center for Environmental Research and Technology, College of Engineering, University of California, Riverside (CE-CERT/UCR). RH inside the chamber was maintained at or below 0.1% RH during dry experiments. In humid experiments, water vapor was generated by bubbling purified air through distilled water and then passing the air through a 1 μ m particle filter; RH was monitored using a LI-COR[®] LI-840A CO_2/H_2O analyzer. Additional details of the chamber facility, aerosol formation yield, and experimental protocols are described in Tang et al. (2013).

A series of chemical and physical characterization instruments were used for the study of aerosol properties. A custom-built scanning mobility particle sizer (SMPS) was used to monitor real-time particle number and volume size (27–685 nm) distributions (Cocker et al., 2001). Total aerosol mass concentration was also calculated by combining time series of volume and aerosol density.

Particle mobility density (ρ) was measured using the coupled aerosol particle mass analyzer (APM) (Kanomax model 3600) and SMPS. In general, aerosol density was determined from the mass selected by the APM and the peak diameter from the SMPS located directly downstream of the APM. Density data were acquired every 75 s. Details of the instruments and theory are described elsewhere (Malloy et al., 2009a; Ehara et al., 1996).

A volatility tandem differential mobility analyzer (VT-DMA) was also custom built and used for online volatility measurement. The VTDMA consists of two differential mobility analyzers (DMA), one condensational particle counter (CPC) and one Dekati[®] thermodenuder (TD, residence time ~ 17 s). The first DMA size-selects particles that transmit through the TD with diameter D_i , while the second DMA and CPC measure the diameter of particles coming out of the TD (D_f) by fitting a log-normal size distribution curve. Volume fraction remaining (VFR) is calculated as the volume ratio of particles before and after passing through the TD with temperature T , i.e., $VFR = (D_f/D_i)^3$.

Chemical composition of chamber SOA was measured with an Aerodyne high-resolution time-of-flight aerosol mass spectrometer (HR-ToF-AMS) (DeCarlo et al., 2006; Jimenez et al., 2003). Non-refractory chemical species in the aerosol phase can be quantified, providing chemistry information of bulk aerosol as well as elemental composition. A particle-into-liquid sampler coupled to dual ion chromatographs (PILS-IC) quantified the particle phase inorganic salts. The configuration of the PILS-IC is described elsewhere (Orsini et al., 2003; Weber et al., 2001).

The CCN activity and supersaturated hygroscopicity is measured with a Droplet Measurement Technologies (DMT) continuous-flow streamwise thermal gradient CCN counter (CFSTGC) (Lance et al., 2006; Roberts and Nenes, 2005). Aerosol from the chamber was classified by a commercial SMPS (TSI 3080), followed in parallel by a CPC (TSI 3772) and the DMT CCN counter. The total aerosol concentration (CN) of the monodisperse particles was counted by the CPC, and the CCN concentration was measured by the CCN counter. The DMA used with the CCN counter was operated at a sheath-to-aerosol flow ratio of 10 : 1. Instrument supersaturation (ss) settings used in this study ranged from 0.2 to 1 % and were calibrated using atomized $(\text{NH}_4)_2\text{SO}_4$ aerosol. Scanning mobility CCN analysis (SMCA) (Moore et al., 2010) provides size-resolved CCN activity using data from the CCN counter and SMPS. By keeping constant instrument ss during the scanning cycle of the SMPS, we obtain the time series of CN and CCN counts, and then use an inversion procedure to determine the CCN/CN ratio as a function of dry mobility diameter. The critical diameter, d_{p50} , corresponding to the CCN/CN ratio of 0.5, is determined for each ss. This procedure is repeated over multiple ss, giving a characterization of the size-resolved CCN properties every 135 s.

3 Theory

3.1 Temperature considerations for CCN measurement

Temperature settings of the DMT CCN counter can affect the CCN activity of volatile aerosol species (Asa-Awuku et al., 2009; Moore and Nenes, 2009; Romakkaniemi et al., 2013). The centerline ss of the CCN counter is controlled by the flow rate (Q) and temperature difference (ΔT) between the top (T_1) and bottom (T_3) at constant column absolute pressure (Fig. S1 in the Supplement, Eq. (6); Roberts and Nenes, 2005). Selecting a linear combination of Q and ΔT will maintain the same or very similar instrument ss. In standard operation, the change of ss is achieved by keeping constant inlet flow rate (0.5 L min^{-1}) and varying ΔT . T_1 (temperature at the top of the column) is identical to the aerosol sample temperature and is constant for all experiments. Therefore the change of ΔT is determined by that of T_3 , temperature at the bottom of the column. Larger temperature gradients along the CCN column are required for higher ss at a constant flow rate, Q . For high ss (e.g., $> 1.0\%$), temperatures at the exit of the DMT CCN column can exceed 35°C . To examine measurement artifacts induced by high temperatures, the temperature gradient inside the CCN column will be varied while keeping the centerline ss constant.

$$\text{ss} \propto \frac{\Delta T}{Q} \quad (1)$$

3.2 κ of multicomponent aerosol system

We use the κ -Köhler theory (Petters and Kreidenweis, 2007) to convert the measured activation diameters to the single hygroscopicity parameter, κ , using the equations as follows:

$$\kappa = \frac{4A^3}{27 \ln^2 S_c d_{p50}^3}, \quad (2)$$

$$A = \frac{4M_w \sigma_w}{RT \rho_w}, \quad (3)$$

where M_w and ρ_w are the molecular weight and density of water, respectively; R the universal gas constant; and T , the ambient temperature. κ -Köhler theory assumes the surface tension of the droplet is that of pure water, $\sigma_w = 0.072 \text{ N m}^{-1}$. S_c is the critical saturation for a dry particle of diameter d_{p50} determined with the SMCA.

For multicomponent aerosol systems, the Zdanovskii, Stokes, and Robinson (ZSR) (Zdanovskii, 1984; Stokes and Robinson, 1966) mixing rule can be applied to predict the CCN activity. ZSR assumes that water uptake by each individual component of a particle is independent and additive. Therefore, the overall κ value is the sum of κ of each individual component weighted by its volume contribution to the total aerosol. We assume two components, including inorganic and organic in the aerosol phase of the amine oxidation products. Applying the ZSR, the κ value of the bulk aerosol can

be estimated as follows (Petters and Kreidenweis, 2007):

$$\kappa = \sum_i \varepsilon_i \kappa_i = \varepsilon_s \kappa_s + \varepsilon_o \kappa_o, \quad (4)$$

where ε_i is the volume (V_i) fraction of the inorganic/organic components in the total aerosol; “s” and “o” subscripts refer to salt (inorganic) and organic components, respectively. ε_s is calculated from the mass fraction, m , and density, ρ , as

$$\varepsilon_s = \frac{V_s}{V_s + V_o} = \frac{m_s / \rho_s}{m_s / \rho_s + m_o / \rho_o}, \quad (5)$$

$$\varepsilon_o = 1 - \varepsilon_s. \quad (6)$$

4 Results and discussion

4.1 Trimethylamine (TMA)

The reaction of TMA with OH and N_2O_5 can form aerosol of varied hygroscopicity and CCN activity. TMA photooxidation with OH in the absence of NO_x formed organic aerosol with low hygroscopicity, $\kappa \sim 0.18$ (Table 1). Similarly, dry reactions between TMA and N_2O_5 produced organic-dominant (total aerosol salt mass fraction, ε_s , < 10 %) secondary aerosol with comparable hygroscopicity ($\kappa \sim 0.20$, Table 1). In humid experiments, nitric acid produced by N_2O_5 and NO_3 can be directly neutralized by TMA and first-generation aerosol products to form inorganic salts (Tang et al., 2013). PILS-IC data confirmed the presence of TMA^+ , DMA^+ , MA^+ , and NO_3^- ions in the aerosol phase. The ε_s was observed to stabilize at ~ 0.15 after 2 h of reaction at RH $\sim 22\%$ (Tang et al., 2013). The CCN activity of the aerosol formed at RH $\sim 22\%$ has $\kappa \sim 0.28$ due to the increased ε_s over the dry experiment, higher than that of the aerosol only composed of organic species.

The difference in single-parameter hygroscopicity is consistent with a two-component (organic and inorganic component) model of κ additivity. The CCN activity of organic components in the multicomponent TMA aerosol is estimated by applying the ZSR mixing rule with κ -Köhler theory. As the concentration of TMA^+ exceeds the sum of methyl and dimethyl amine ions (MA^+ and DMA^+), the inorganic components properties are assumed similar to those of $C_3H_9N \cdot HNO_3$. Table 2 shows the measured κ value, density, mass fraction, and calculated volume fraction of $C_3H_9N \cdot HNO_3$. The calculated κ value for organic components in the humid TMA- NO_3 aerosol is 0.19, similar to that of the dry TMA- NO_3 aerosol. Despite the presence of a potential salt-forming reaction pathway under humid conditions, the mechanism for TMA SOA resulted in materials with similar hygroscopicity to those formed under dry conditions.

Comparison of the VFR of TMA- NO_3 secondary aerosols indicates subtle differences in the organic species formed in dry and humid reactions (Fig. 1b and Table 1). Of the aerosol

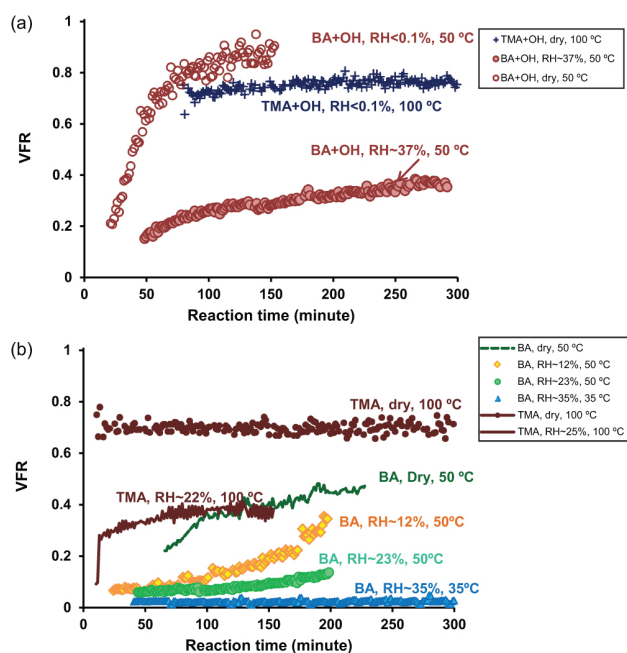


Figure 1. Volume fraction remaining (VFR) of secondary aerosol formed from (a) OH photooxidation and (b) amine- N_2O_5 reactions. For TMA aerosols, VTDMA temperature was set to be 100 °C, while for BA 50 °C or 35 °C because of their higher volatility.

formed, the VFR is 70 % for the TMA- N_2O_5 aerosol in the dry experiment after ~ 17 s exposure at 100 °C in the VT-DMA. As RH and salt fraction increase, the aerosol becomes more volatile; $\sim 40\%$ of the TMA- N_2O_5 aerosol formed at RH $\sim 22\%$ remains, suggesting that the evaporated aerosol has doubled in volume. From our current knowledge of nitrate salts, the aminium salts formed are likely volatile. The equilibrium constant between NH_3 , HNO_3 , and NH_4NO_3 determines a very high vapor pressure of NH_4NO_3 at ambient temperature (Stelson and Seinfeld, 1982a, b; Stelson et al., 1979). Assuming the inorganic salts (volume fraction 16.5 % in total aerosol) evaporate completely at 100 °C, the aerosol will lead to a difference of 0.165 in the VFR instead of ~ 0.3 . In conclusion, “humid” organic aerosol is more volatile than dry TMA- N_2O_5 organic aerosol, despite similar hygroscopicity.

4.2 Butylamine (BA)

Hygroscopicity of BA secondary aerosols formed in dry and humid (RH $\sim 36\%$) OH photooxidation experiments are comparable to TMA aerosols (0.23 ± 0.01 vs. 0.25 ± 0.03 , Table 1). However, the volatility of humid aerosol is notably higher than that of dry aerosol at $T = 50$ °C (Fig. 1a). BA secondary aerosol formed in higher RH is another example of aerosol with similar CCN activity possessing dissimilar volatility.

Table 1. κ and VFR values of aerosol formed from reactions with OH (H_2O_2 as source), NO_3 (N_2O_5 as source), and HNO_3 . The range of VFR is shown (e.g., 0.21–0.91) when standard deviation exceeds 0.06.

Amine	Oxidant	RH (%)	κ	VTDMA temp ($^\circ\text{C}$)	VFR
TMA	H_2O_2	<0.1	0.18 ± 0.02	100	$0.75 \pm 0.02^*$
		30	N/A		
	N_2O_5	<0.1	0.20 ± 0.02	100	$0.7 \pm 0.02^*$
		~ 25	0.28 ± 0.02	100	$0.38 \pm 0.02^*$
BA	H_2O_2	<0.1	0.23 ± 0.01	50	0.21–0.91
		~ 37	0.25 ± 0.03	50	0.16–0.38
	N_2O_5	<0.1	0.19 ± 0.04	50	0.22–0.48
		12	0.48 ± 0.10	50	0.07–0.35
		23	0.33 ± 0.08	50	0.06–0.14
		30	0.49 ± 0.08		
35	0.60 ± 0.10	35	$0.03 \pm 0.01^*$		
$\text{C}_3\text{H}_9\text{N} \cdot \text{HNO}_3$			0.72 ± 0.04		
$\text{C}_4\text{H}_{11}\text{N} \cdot \text{HNO}_3$			0.53 ± 0.03	35	$0.10 \pm 0.06^*$
NH_4NO_3			0.74		

* Average \pm standard deviation.**Table 2.** Mass and volume fraction, density, and hygroscopicity of inorganic/organic components in the humid (RH $\sim 22\%$) TMA– NO_3 aerosol.

	Mass fraction	Density (g cm^{-3})	Volume fraction	Hygroscopicity parameter
	m	ρ	ε	κ
Salt	0.15	1.25*	0.165	0.72 ± 0.02
Organics	0.85	1.40**	0.835	0.19 ± 0.00
Bulk aerosol	1		1	0.28 ± 0.02

* Salo et al. (2011).

** Tang et al. (2013).

BA secondary aerosols formed from reactions with N_2O_5 were more volatile than OH photooxidation SOA while susceptible to changes in temperature as well. We compared the VFR and hygroscopicity of BA– N_2O_5 aerosol formed under four different relative humidity (RH < 0.1 %, $\sim 12\%$, $\sim 23\%$ and $\sim 35\%$). BA– N_2O_5 aerosol formed at RH < 0.1 % (i.e., dry) has VFR < 0.5 at 50°C , which is much more volatile than the TMA– N_2O_5 aerosol. Nevertheless, hygroscopicity of dry BA– N_2O_5 aerosol is similar to that of dry TMA– N_2O_5 aerosol, corresponding to the chemical nature of organic-dominant secondary aerosols.

As with TMA, increasing RH forms more aminium salts in the aerosol phase and increased volatility and CCN activity of BA secondary aerosol systems. Higher concentrations of water vapor enhanced the salt-forming pathways (e.g., the formation of nitric acid) such that significant amounts of inorganic salts formed in the humid experiments. Other than butylaminium nitrate ($\text{C}_4\text{H}_{11}\text{N} \cdot \text{HNO}_3$) via direct re-

action of BA + HNO_3 , additional pathways lead to the formation of another salt, ammonium nitrate (NH_4NO_3). Figure 2 shows the ratio of mass concentration ($\mu\text{g m}^{-3}$) of two cations, NH_4^+ and BA^+ , in the total BA aerosol mass concentration ($\mu\text{g m}^{-3}$) using data collected by PILS-IC and SMPS. With higher RH, the relative contribution of ammonium ion (NH_4^+) in the total aerosol increased, while that of butylaminium ion (BA^+) follows the opposite trend. As the κ value of NH_4NO_3 is larger than that of $\text{C}_4\text{H}_{11}\text{N} \cdot \text{HNO}_3$ (0.74 vs. 0.53, Table 1), aerosol containing more NH_4NO_3 exhibited reasonably higher CCN activity. Similarly, higher volatility is observed with the elevation of RH and mass fraction of NH_4NO_3 in the BA– N_2O_5 reactions (Fig. 1b). As mentioned in Sect. 4.1, NH_4NO_3 has high vapor pressure even at ambient temperature, and the partitioning between particle and gas phase is a strong function of temperature and relative humidity. $\text{C}_4\text{H}_{11}\text{N} \cdot \text{HNO}_3$ particles formed from BA and HNO_3 in the same chamber reactor are also volatile, with VFR < 0.1 at VTDMA $T = 35^\circ\text{C}$, which is similar to that of humid BA– N_2O_5 aerosol formed at 35 % RH (Fig. 1b). Thus, higher relative humidity promotes the partitioning of BA secondary aerosol from particle phase to gas phase.

As CCN activity of humid BA– NO_3 aerosols is elevated by the presence of inorganic salts, the variability of κ values increases notably compared with that of dry aerosol and is greater than TMA secondary aerosol as well. In addition to time-dependent aerosol CCN activity, measured κ values varied with changes of ss setting. Figure 3 shows the time series of κ values measured at different ss ranging from 0.23 to 0.87 % for the BA– N_2O_5 reaction at RH $\sim 30\%$. Briefly, κ measured at higher ss (i.e., the ss settings > 0.4 %) was

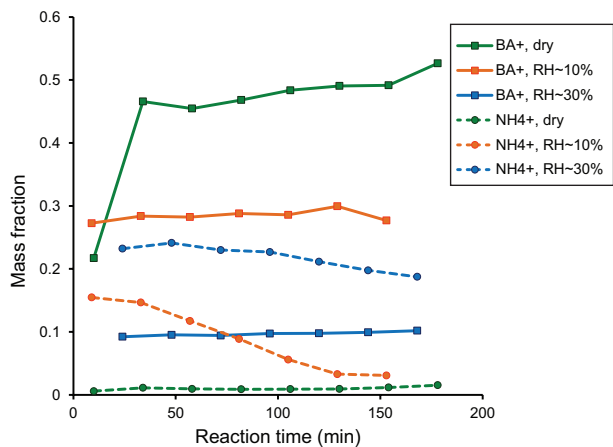


Figure 2. Fraction of BA^+ and NH_4^+ mass measured by PILS-IC in the total aerosol mass for the $\text{BA} + \text{N}_2\text{O}_5$ experiments under three different relative humidities ($\text{RH} < 0.1\%$, 10% , 30%).

smaller than those measured at lower *ss* (i.e., the *ss* settings $\leq 0.4\%$), and the discrepancy was observed from the beginning to the end of the experiment. As defined in Peters and Kreidenweis (2007), the hygroscopicity parameter κ is only dependent on aerosol composition, not on the value of *ss*. Therefore, there are likely differences in the aerosol solute composition measured at high and low *ss*. To avoid the influence of relative humidity while examining the effect of temperature on the CCN activity measurement, similar *ss* ($\sim 0.38\%$) was achieved by adjusting the temperature difference (ΔT) and flow rate (Q) as discussed in the theory section. It is to be noted that residence time of sampled aerosol was extended under the higher ΔT and lower Q conditions.

Aerosol formed from humid ($\text{RH} \sim 30\%$) experiments between BA and NO_3 were re-examined using the same CCN counter with varying temperature difference (ΔT) of the CCN column listed in Table 3. Calculated κ values were shown in Fig. 4. κ measured at $\Delta T = 7, 14$ and 17°C are consistent, with standard deviation ± 0.04 , and show a slight decrease at the beginning of the experiments. However, when $\Delta T = 21^\circ\text{C}$ and $Q = 167\text{ cm}^3\text{ min}^{-1}$, it is not possible to determine the critical diameter needed for calculating κ ; the CCN/CN ratio for all sizes from 10 to 250 nm was below 0.2, and the activation curve did not reach a plateau typical of CCN-active aerosol. BA aerosol was unable to fully activate inside the CCN column as a result of the high temperature and longer residence time. High temperature favors particle–gas-phase partitioning, and both $\text{C}_4\text{H}_{11}\text{N} \cdot \text{HNO}_3$ and NH_4NO_3 are water-soluble, which may incur more material losses to the CCN column wall during the longer retention time inside the CCN column. Thus, a shrinking particle size caused by evaporation and dissolution of volatile compounds is assumed to be responsible for the failure of activation. However, the measured CCN activity of dry $\text{C}_4\text{H}_{11}\text{N} \cdot \text{HNO}_3$ and NH_4NO_3 particles may

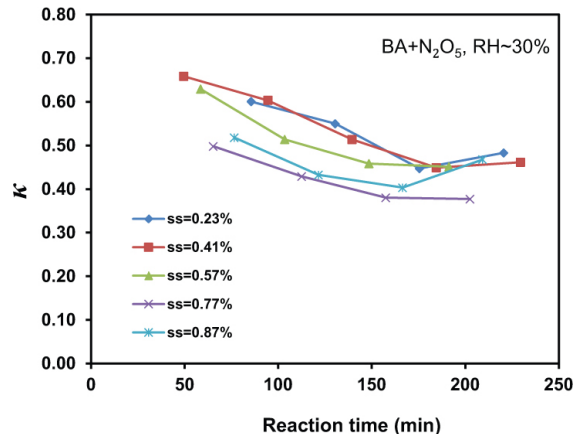


Figure 3. κ measured at different *ss* showed inconsistency for secondary aerosol formed from $\text{BA} + \text{N}_2\text{O}_5$ at $\text{RH} \sim 30\%$.

Table 3. Values of temperature difference (ΔT), flow rate (Q), and the corresponding *ss* (%) from $(\text{NH}_4)_2\text{SO}_4$ calibration of the CCN counter.

ΔT ($^\circ\text{C}$)	Flow rate, Q ($\text{cm}^3\text{ min}^{-1}$)	<i>ss</i> (%)	$(\text{NH}_4)_2\text{SO}_4$ d_{p50} (nm)
7	500	0.37	53.05
14	250	0.39	49.69
17	206	0.38	50.85
21	167	0.37	51.46

be less sensitive to temperature change of the CCN counter column during the measurement. No distinct difference between critical diameters measured with $\Delta T = 7$ and 21°C was observed for dry atomized NH_4NO_3 aerosol, as well as $\text{C}_4\text{H}_{11}\text{N} \cdot \text{HNO}_3$ particles, for which only a 10% difference of κ was discovered. It implies that even low RH ($\sim 30\%$) can modify the BA secondary aerosol gas-to-particle partitioning, which is amplified when exposed to supersaturated conditions.

5 Summary and conclusions

The formation of aliphatic amine secondary aerosol is complex and the reaction pathways can lead to the formation of organic and inorganic components. Changes in the single hygroscopicity parameter κ reflect changes in aerosol chemical composition. The CCN activity for amine secondary aerosol is dependent on the reaction pathways. N_2O_5 -initiated reaction pathways produce more CCN-active aerosol than in OH radical systems, especially in humid conditions. The tertiary amine precursors form less volatile materials that can be described by a two-component additive (inorganic/organic) hygroscopicity model. Variability in amine hygroscopicity, especially for primary aliphatic amines, is due to the presence of volatile components. Tertiary aerosol does not exhibit

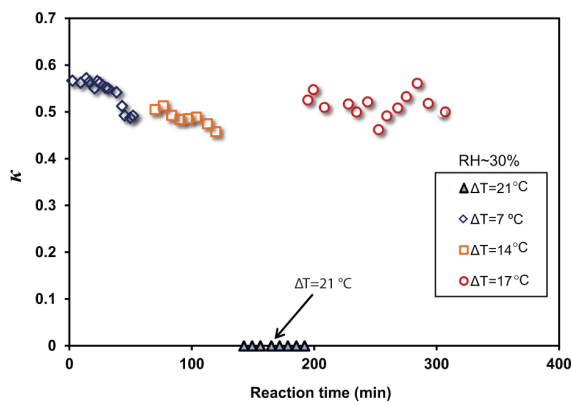


Figure 4. Measured κ values at $ss \sim 0.38\%$ for butylamine (BA) + N_2O_5 aerosol formed at $RH \sim 30\%$. Symbols represent various temperature difference (ΔT) between the top and bottom of the CCN counter column.

variability in hygroscopicity, while primary aliphatic amine aerosol is more susceptible to changes in temperature and RH.

The formation of salts will increase CCN activity. The behavior of BA aerosol within the CCN counter suggests that aerosol formed at lower RH may modify gas–particle partitioning if exposed to increasing RH. Hence as RH increases in a parcel of air, the composition of secondary amine aerosol may become more CCN active. Because of their notable aerosol yield and the potential impacts on cloud formation and global climate, further study is required to understand the ambient nature of aliphatic amines. Specifically the vertical distribution of inorganic–organic partitioning of the aerosol from the surface to cloud-top altitudes should be investigated.

Furthermore, the time of day of aerosol formation must also be considered. OH and NO_3 reactions representative of daytime versus nighttime reactions produce aerosol of varied salt content and hence CCN activity. Nighttime secondary aliphatic amine atmospheric reactions are likely to promote the formation of hygroscopic material that can induce low-level clouds and fogs. Thus, the contribution of amines to regional CCN is complex and requires additional controlled exploratory efforts.

Acknowledgements. This work was supported in part by the National Science Foundation (ENG 1032388 & ATM 0849765) and W. M. Keck Foundation. D. Vu acknowledges US Environmental Protection Agency (EPA) STAR Fellowship Assistance Agreement no. FP-91751101 for her contribution to this work. Any opinions, findings, and conclusions expressed in this material are those of the author(s) and do not necessarily reflect the views of the NSF or EPA. No endorsement is implied by the USDA for any instrument or method mentioned here to the exclusion of other methods which provide similar ability.

Edited by: A. Virtanen

References

- Asa-Awuku, A., Engelhart, G. J., Lee, B. H., Pandis, S. N., and Nenes, A.: Relating CCN activity, volatility, and droplet growth kinetics of β -caryophyllene secondary organic aerosol, *Atmos. Chem. Phys.*, 9, 795–812, doi:10.5194/acp-9-795-2009, 2009.
- Asa-Awuku, A., Moore, R. H., Nenes, A., Bahreini, R., Holloway, J. S., Brock, C. A., Middlebrook, A. M., Ryerson, T. B., Jimenez, J. L., DeCarlo, P. F., Hecobian, A., Weber, R. J., Stickel, R., Tanner, D. J., and Huey, L. G.: Airborne cloud condensation nuclei measurements during the 2006 Texas Air Quality Study, *J. Geophys. Res.-Atmos.*, 116, D11201, doi:10.1029/2010jd014874, 2011.
- Berndt, T., Stratmann, F., Sipilä, M., Vanhanen, J., Petäjä, T., Mikkilä, J., Grünner, A., Spindler, G., Lee Mauldin III, R., Curtius, J., Kulmala, M., and Heintzenberg, J.: Laboratory study on new particle formation from the reaction $OH + SO_2$: influence of experimental conditions, H_2O vapour, NH_3 and the amine tert-butylamine on the overall process, *Atmos. Chem. Phys.*, 10, 7101–7116, doi:10.5194/acp-10-7101-2010, 2010.
- Cocker, D. R., Flagan, R. C., and Seinfeld, J. H.: State-of-the-art chamber facility for studying atmospheric aerosol chemistry, *Environ. Sci. Technol.*, 35, 2594–2601, 2001.
- DeCarlo, P. F., Kimmel, J. R., Trimborn, A., Northway, M. J., Jayne, J. T., Aiken, A. C., Gonin, M., Fuhrer, K., Horvath, T., Docherty, K. S., Worsnop, D. R., and Jimenez, J. L.: Field-deployable, high-resolution, time-of-flight aerosol mass spectrometer, *Anal. Chem.*, 78, 8281–8289, doi:10.1021/ac061249n, 2006.
- Dusek, U., Frank, G. P., Hildebrandt, L., Curtius, J., Schneider, J., Walter, S., Chand, D., Drewnick, F., Hings, S., Jung, D., Borrmann, S., and Andreae, M. O.: Size matters more than chemistry for cloud-nucleating ability of aerosol particles, *Science*, 312, 1375–1378, 2006.
- Ehara, K., Hagwood, C., and Coakley, K. J.: Novel method to classify aerosol particles according to their mass-to-charge ratio – Aerosol particle mass analyser, *J. Aerosol. Sci.*, 27, 217–234, 1996.
- Finlayson-Pitts, B. J. and Pitts, J. N. J.: *Atmospheric chemistry. Fundamentals and experimental techniques*, John Wiley & Sons, New York, NY, USA, 1098 pp., 1986.
- Fitzgerald, J. W., Hoppel, W. A., and Vietti, M. A.: The Size and Scattering Coefficient of Urban Aerosol-Particles at Washington, Dc as a Function of Relative-Humidity, *J. Atmos. Sci.*, 39, 1838–1852, 1982.
- Ge, X. L., Wexler, A. S., and Clegg, S. L.: Atmospheric amines – Part I. A review, *Atmos. Environ.*, 45, 524–546, 2011a.
- Ge, X. L., Wexler, A. S., and Clegg, S. L.: Atmospheric amines - Part II. Thermodynamic properties and gas/particle partitioning, *Atmos. Environ.*, 45, 561–577, 2011b.
- Glagolenko, S. and Phares, D. J.: Single-particle analysis of ultra-fine aerosol in College Station, Texas, *J. Geophys. Res.-Atmos.*, 109, D18205, doi:10.1029/2004jd004621, 2004.
- Gray, H. A., Cass, G. R., Huntzicker, J. J., Heyerdahl, E. K., and Rau, J. A.: Characteristics of Atmospheric Organic and Elemental Carbon Particle Concentrations in Los-Angeles, *Environ. Sci. Technol.*, 20, 580–589, 1986.
- Hudson, J. G. and Da, X. Y.: Volatility and size of cloud condensation nuclei, *J. Geophys. Res.-Atmos.*, 101, 4435–4442, 1996.
- Jimenez, J. L., Jayne, J. T., Shi, Q., Kolb, C. E., Worsnop, D. R., Yourshaw, I., Seinfeld, J. H., Flagan, R. C., Zhang, X. F., Smith, K. A., Morris, J. W., and Davidovits, P.: Ambient aerosol

- sampling using the Aerodyne Aerosol Mass Spectrometer, *J. Geophys. Res.-Atmos.*, 108, 8425, doi:10.1029/2001jd001213, 2003.
- Jimenez, J. L., Canagaratna, M. R., Donahue, N. M., Prevot, A. S. H., Zhang, Q., Kroll, J. H., DeCarlo, P. F., Allan, J. D., Coe, H., Ng, N. L., Aiken, A. C., Docherty, K. S., Ulbrich, I. M., Grieshop, A. P., Robinson, A. L., Duplissy, J., Smith, J. D., Wilson, K. R., Lanz, V. A., Hueglin, C., Sun, Y. L., Tian, J., Laaksonen, A., Raatikainen, T., Rautiainen, J., Vaattovaara, P., Ehn, M., Kulmala, M., Tomlinson, J. M., Collins, D. R., Cubison, M. J., Dunlea, E. J., Huffman, J. A., Onasch, T. B., Alfarra, M. R., Williams, P. I., Bower, K., Kondo, Y., Schneider, J., Drewnick, F., Borrmann, S., Weimer, S., Demerjian, K., Salcedo, D., Cottrell, L., Griffin, R., Takami, A., Miyoshi, T., Hatakeyama, S., Shimojo, A., Sun, J. Y., Zhang, Y. M., Dzepina, K., Kimmel, J. R., Sueper, D., Jayne, J. T., Herndon, S. C., Trimborn, A. M., Williams, L. R., Wood, E. C., Middlebrook, A. M., Kolb, C. E., Baltensperger, U., and Worsnop, D. R.: Evolution of organic aerosols in the atmosphere, *Science*, 326, 1525–1529, 2009.
- Kanakidou, M., Seinfeld, J. H., Pandis, S. N., Barnes, I., Dentener, F. J., Facchini, M. C., Van Dingenen, R., Ervens, B., Nenes, A., Nielsen, C. J., Swietlicki, E., Putaud, J. P., Balkanski, Y., Fuzzi, S., Horth, J., Moortgat, G. K., Winterhalter, R., Myhre, C. E. L., Tsigaridis, K., Vignati, E., Stephanou, E. G., and Wilson, J.: Organic aerosol and global climate modelling: a review, *Atmos. Chem. Phys.*, 5, 1053–1123, doi:10.5194/acp-5-1053-2005, 2005.
- Lance, S., Medina, J., Smith, J. N., and Nenes, A.: Mapping the operation of the DMT Continuous Flow CCN counter, *Aerosol. Sci. Tech.*, 40, 242–254, 2006.
- Loukonen, V., Kurtén, T., Ortega, I. K., Vehkamäki, H., Pádua, A. A. H., Sellegri, K., and Kulmala, M.: Enhancing effect of dimethylamine in sulfuric acid nucleation in the presence of water – a computational study, *Atmos. Chem. Phys.*, 10, 4961–4974, doi:10.5194/acp-10-4961-2010, 2010.
- Malloy, Q. G. J., Nakao, S., Qi, L., Austin, R., Stothers, C., Hagino, H., and Cocker, D. R.: Real-Time Aerosol Density Determination Utilizing a Modified Scanning Mobility Particle Sizer Aerosol Particle Mass Analyzer System, *Aerosol. Sci. Tech.*, 43, 673–678, 2009a.
- Malloy, Q. G. J., Li Qi, Warren, B., Cocker III, D. R., Erupe, M. E., and Silva, P. J.: Secondary organic aerosol formation from primary aliphatic amines with NO₃ radical, *Atmos. Chem. Phys.*, 9, 2051–2060, doi:10.5194/acp-9-2051-2009, 2009b.
- Mikhailov, E., Vlasenko, S., Rose, D., and Pöschl, U.: Mass-based hygroscopicity parameter interaction model and measurement of atmospheric aerosol water uptake, *Atmos. Chem. Phys.*, 13, 717–740, doi:10.5194/acp-13-717-2013, 2013.
- Moore, R. H. and Nenes, A.: Scanning Flow CCN Analysis-A Method for Fast Measurements of CCN Spectra, *Aerosol Sci. Tech.*, 43, 1192–1207, 2009.
- Moore, R. H., Nenes, A., and Medina, J.: Scanning Mobility CCN Analysis-A method for fast measurements of size-resolved CCN distributions and activation kinetics, *Aerosol. Sci. Tech.*, 44, 861–871, doi:10.1080/02786826.2010.498715, 2010.
- Moore, R. H., Raatikainen, T., Langridge, J. M., Bahreini, R., Brock, C. A., Holloway, J. S., Lack, D. A., Middlebrook, A. M., Perring, A. E., Schwarz, J. P., Spackman, J. R., and Nenes, A.: CCN Spectra, Hygroscopicity, and Droplet Activation Kinetics of Secondary Organic Aerosol Resulting from the 2010 Deep-water Horizon Oil Spill, *Environ. Sci. Technol.*, 46, 3093–3100, doi:10.1021/es203362w, 2012.
- Murphy, S. M., Sorooshian, A., Kroll, J. H., Ng, N. L., Chhabra, P., Tong, C., Surratt, J. D., Knipping, E., Flagan, R. C., and Seinfeld, J. H.: Secondary aerosol formation from atmospheric reactions of aliphatic amines, *Atmos. Chem. Phys.*, 7, 2313–2337, doi:10.5194/acp-7-2313-2007, 2007.
- Orsini, D. A., Ma, Y. L., Sullivan, A., Sierau, B., Baumann, K., and Weber, R. J.: Refinements to the particle-into-liquid sampler (PILS) for ground and airborne measurements of water soluble aerosol composition, *Atmos. Environ.*, 37, 1243–1259, 2003.
- Petters, M. D. and Kreidenweis, S. M.: A single parameter representation of hygroscopic growth and cloud condensation nucleus activity, *Atmos. Chem. Phys.*, 7, 1961–1971, doi:10.5194/acp-7-1961-2007, 2007.
- Rabaud, N. E., Ebeler, S. E., Ashbaugh, L. L., and Flocchini, R. G.: Characterization and quantification of odorous and non-odorous volatile organic compounds near a commercial dairy in California, *Atmos. Environ.*, 37, 933–940, 2003.
- Rehbein, P. J. G., Jeong, C. H., McGuire, M. L., Yao, X. H., Corbin, J. C., and Evans, G. J.: Cloud and Fog Processing Enhanced Gas-to-Particle Partitioning of Trimethylamine, *Environ. Sci. Technol.*, 45, 4346–4352, doi:10.1021/es1042113, 2011.
- Roberts, G. C. and Nenes, A.: A continuous-flow streamwise thermal-gradient CCN chamber for atmospheric measurements, *Aerosol Sci. Tech.*, 39, 206–221, 2005.
- Rogge, W. F., Mazurek, M. A., Hildemann, L. M., Cass, G. R., and Simoneit, B. R. T.: Quantification of Urban Organic Aerosols at a Molecular-Level – Identification, Abundance and Seasonal-Variation, *Atmos. Environ. A-Gen.*, 27, 1309–1330, 1993.
- Romakkaniemi, S., Jaatinen, A., Laaksonen, A., Nenes, A., and Raatikainen, T.: The effect of phase partitioning of semivolatile compounds on the measured CCN activity of aerosol particles, *Atmos. Meas. Tech. Discuss.*, 6, 8413–8433, doi:10.5194/amtd-6-8413-2013, 2013.
- Saxena, P. and Hildemann, L.: Water-soluble organics in atmospheric particles: A critical review of the literature and application of thermodynamics to identify candidate compounds, *J. Atmos. Chem.*, 24, 57–109, doi:10.1007/bf00053823, 1996.
- Silva, P. J., Erupe, M. E., Price, D., Elias, J., Malloy, Q. G. J., Li, Q., Warren, B., and Cocker, D. R., III: Trimethylamine as precursor to secondary organic aerosol formation via nitrate radical reaction in the atmosphere, *Environ. Sci. Technol.*, 42, 4689–4696, doi:10.1021/es703016v, 2008.
- Sorooshian, A., Murphy, S. M., Hersey, S., Gates, H., Padro, L. T., Nenes, A., Brechtel, F. J., Jonsson, H., Flagan, R. C., and Seinfeld, J. H.: Comprehensive airborne characterization of aerosol from a major bovine source, *Atmos. Chem. Phys.*, 8, 5489–5520, doi:10.5194/acp-8-5489-2008, 2008.
- Stelson, A. W. and Seinfeld, J. H.: Relative humidity and pH dependence of the vapor pressure of ammonium nitrate-nitric acid solutions at 25 °C, *Atmos. Environ.*, 16, 993–1000, doi:10.1016/0004-6981(82)90185-8, 1982a.
- Stelson, A. W. and Seinfeld, J. H.: Relative humidity and temperature dependence of the ammonium nitrate dissociation constant, *Atmos. Environ.*, 16, 983–992, doi:10.1016/0004-6981(82)90184-6, 1982b.

- Stelson, A. W., Friedlander, S. K., and Seinfeld, J. H.: A note on the equilibrium relationship between ammonia and nitric acid and particulate ammonium nitrate, *Atmos. Environ.*, 13, 369–371, doi:10.1016/0004-6981(79)90293-2, 1979.
- Stokes, R. H. and Robinson, R. A.: Interactions in Aqueous Nonelectrolyte Solutions. I. Solute-Solvent Equilibria, *J. Phys. Chem.*, 70, 2126–2131, doi:10.1021/j100879a010, 1966.
- Tang, X., Cocker III, D. R., and Asa-Awuku, A.: Are sesquiterpenes a good source of secondary organic cloud condensation nuclei (CCN)? Revisiting β -caryophyllene CCN, *Atmos. Chem. Phys.*, 12, 8377–8388, doi:10.5194/acp-12-8377-2012, 2012.
- Tang, X., Price, D., Praske, E., Lee, S. A., Shattuck, M. A., Purvis-Roberts, K., Silva, P. J., Asa-Awuku, A., and Cocker III, D. R.: NO_3 radical, OH radical and O_3 -initiated secondary aerosol formation from aliphatic amines, *Atmos. Environ.*, 72, 105–112, doi:10.1016/j.atmosenv.2013.02.024, 2013.
- Wang, L., Khalizov, A. F., Zheng, J., Xu, W., Ma, Y., Lal, V., and Zhang, R. Y.: Atmospheric nanoparticles formed from heterogeneous reactions of organics, *Nat. Geosci.*, 3, 238–242, 2010a.
- Wang, L., Lal, V., Khalizov, A. F., and Zhang, R. Y.: Heterogeneous Chemistry of Alkylamines with Sulfuric Acid: Implications for Atmospheric Formation of Alkylammonium Sulfates, *Environ. Sci. Technol.*, 44, 2461–2465, 2010b.
- Weber, R. J., Orsini, D., Daun, Y., Lee, Y. N., Klotz, P. J., and Brechtel, F.: A particle-into-liquid collector for rapid measurement of aerosol bulk chemical composition, *Aerosol Sci. Tech.*, 35, 718–727, 2001.
- Zdanovskii, A. B.: Novyi Metod Rascheta Rastvorimostei Elektrolitov v Mnogokomponentnykh, 20 Sistema, *Zh. Fiz. Khim.*, 22, 1478–1485, 1486–1495, 1948.
- Zhang, G. H., Bi, X. H., Chan, L. Y., Li, L., Wang, X. M., Feng, J. L., Sheng, G. Y., Fu, J. M., Li, M., and Zhou, Z.: Enhanced trimethylamine-containing particles during fog events detected by single particle aerosol mass spectrometry in urban Guangzhou, China, *Atmos. Environ.*, 55, 121–126, doi:10.1016/j.atmosenv.2012.03.038, 2012.